Wind and Structures, Vol. 8, No. 2 (2005) 79-88
DOI: http://dx.doi.org/10.12989/was.2005.8.2.079

Unifying calculation of vortex-induced vibrations of overhead conductors

André Leblond†

Hydro-Québec TransÉnergie, 800, boul. de Maisonneuve Est, 21st Floor, Montréal, Québec H2L 4M8, Canada

Claude Hardy‡

Claude Hardy International Inc., 95 rue Lamarche, St-Bruno, Québec, J3V 5A6, Canada

(Received December 18, 2003, Accepted June 22, 2004)

Abstract. This paper deals with a unified way for calculating vortex-induced vibrations (Aeolian vibrations in transmission line parlance) of undamped single overhead conductors. The main objective of the paper is to identify reduced parameters which would unify the predicted vibration response to the largest possible extent. This is actually done by means of a simple mathematical transformation resulting, for a given terrain (associated to a given wind turbulence intensity), into a single, unified response curve that is applicable to any single multi-layered aluminium conductor. In order to further validate the above process, the predicted, unified response curve is compared with measured response curves drawn from tests run on a full-scale test line using several aluminium-conductor-steel-reinforced (ACSR), all-alloy-aluminium-conductor (AAAC) and aluminium-conductor-alloy-reinforced (ACAR) conductors strung at different tensions. On account of the expected scatter in the results from such field tests, the agreement is shown to be good. The final results are expressed by means of only four different curves pertaining to four different terrain characteristics. These curves may then be used to assess the vibration response of any undamped single, multi-layer aluminium conductor of any diameter, strung at any practical tension.

Keywords: Aeolian vibrations; vortex-induced vibrations; conductors; wind power input; self-damping; energy balance principle.

1. Introduction

Transmission line conductors are subjected to various types of wind-induced motion such as Aeolian vibrations, galloping and wake-induced oscillations. When exposed to light, steady winds, overhead conductors display potentially harmful Aeolian vibrations related to the vortex shedding mechanism. These vibrations are self-limiting so that the conductor's maximum displacement amplitude does not exceed one conductor diameter. However, even such small amplitudes may lead to strand fatigue failures at suspension points. In order to achieve safe vibration conditions, one needs to rely on proper aeroelastic and structural modelling of the system.

Vibration amplitudes are usually determined by means of the so-called Energy Balance Principle

† Research Engineer, Corresponding Author, E-mail: Leblond.Andre.2@hydro.qc.ca
‡ Consultant

(EBP), in which the energy dissipated through conductor self-damping just balances the energy imparted by the wind (EPRI 1979). The straightforward EBP is considered acceptable for line engineering applications of undamped single conductors and a number of computer programs have been written around it to predict conductor vibration amplitudes as a function of frequency. However, any change in mechanical tension, wind turbulence intensity or conductor type requires a new run with the computer program and this gives rise to an updated vibration amplitude curve as a function of frequency. This process soon becomes tedious when several values of these parameters have to be considered.

The main objective of the paper is to identify reduced parameters which would unify the predicted vibration response to the largest possible extent (Leblond and Hardy 2003). This is actually done by means of a simple mathematical transformation presented in the next section.

2. Mathematical analysis

2.1. Wind power input

Vortex-induced vibration of a circular cylinder is a very complex aeroelastic phenomenon affecting particularly overhead transmission lines. Effective wind power imparted to conductors has been the subject of numerous investigations over the last decades. There is considerable dispersion in the published data on wind power input (Brika and Laneville 1996), the difference between various investigators falling within a range of about 2:1. However, wind power input can always be expressed in terms of a reduced decrement δ_r (Rawlins 1982) or a reduced excitation factor η_r (Noiseux, *et al.* 1988) through the relationship:

$$\eta_r = \frac{\delta_r}{\pi} = fnc_1\left(\frac{y_{\max}}{d}, I\right) \tag{1}$$

where $fnc_1\{(y_{\max}/d), I\}$ is a function of both the reduced antinode amplitude $y_{\max}/d$, the ratio of maximum antinode amplitude $y_{\max}$ to conductor diameter d, and wind turbulence intensity I. Wind turbulence intensity I is defined as the ratio of the RMS variation of wind velocity along three mutually perpendicular axes to the magnitude of the mean wind velocity. Eq. (1) is non-linear and determined from wind tunnel experiments at constant wind speed on rigid rods or flexible models, and the resulting data are transformed numerically (Noiseux, *et al.* 1988, Rawlins 1998) to take into account the turbulence intensity I of natural wind. Function fnc_1 can take the form of a family of curves, one for each value of wind turbulence intensity I, where the reduced excitation factor η_r is a function of the reduced antinode amplitude. Typical curves are shown in Fig. 1 (Noiseux, *et al.* 1988).

Wind turbulence arises from the interaction of the mean wind with the ground and its intensity at any particular field location is strongly influenced by the local terrain, and especially the nature of ground cover. Typical values can be approximated for various classes of terrain category as shown in Table 1 (CIGRE SC22-WG11-TF4 1999). Turbulence reduces the amount of wind power imparted to vibrating conductors.

From Eq. (1), the η_r results are used to calculate the actual excitation factor η_w for a vibrating span exposed to wind:

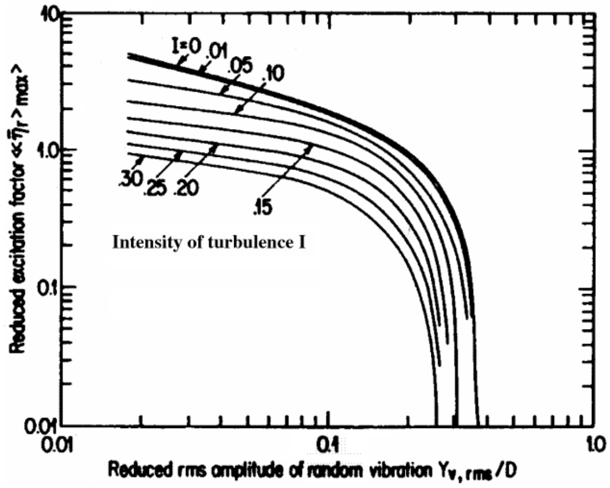

Fig. 1 Reduced excitation factor as a function of reduced RMS amplitude of vibration at constant wind turbulence intensity (Noiseux, *et al.* 1988)

Table 1 Classes of terrain category according to CIGRE SC22-WG11-TF4 (1999)

Terrain category	Terrain characteristics	I	$(H/w)_{\mathrm{adm}}$ (m)
1	Open, flat, no trees, no obstruction, with snow cover, or near/across large bodies of water; flat desert.	0.08	1000
2	Open, flat, no obstruction, no snow; e.g. farmland without any obstruction, summer time.	0.15	1125
3	Open, flat, or undulating with very few obstacles, e.g. open grass or farmland with few trees, hedgerows and other barriers; prairie, tundra.	0.22	1225
4	Built-up with some trees and building, e.g. residential suburbs; small towns; woodlands and shrubs. Small fields with bushes, trees and hedges.	0.30	1425

$$\eta_w = \frac{\rho_a d^2}{2m}\eta_r \tag{2}$$

where ρ_a is the air density, d is the conductor diameter and m is the conductor mass per unit length. Alternatively, the reduced excitation factor η_r can also be converted to power imparted by wind P_w, which is the parameter commonly used by some conductor vibration specialists:

$$\frac{P_w}{L} = \rho_a d^4 f^3 \pi^3 \left(\frac{y_{\max}}{d}\right)^2 \eta_r \tag{3}$$

where f is vibration frequency and L is conductor length. The η_r results may be converted either to η_w by means of Eq. (2) or to P_w using Eq. (3), the proper choice depending mostly upon the form in which information on conductor self-damping is available.

2.2. Conductor self-damping

Conductor self-damping represents the capacity of the conductor to dissipate energy internally while vibrating. It is usually measured on a laboratory test span where the conductor is brought into a sequence of resonance frequencies at a controlled antinode amplitude by means of an electromagnetic shaker (CIGRE SC22 1979, IEEE Standard 563-1978). Self-damping measurements are curve-fitted by means of a power law:

$$\frac{P_c}{L} = K_1 \frac{y_{\max}^{\alpha} f^{\beta}}{T^{\gamma}} \tag{4}$$

in which P_c/L is the power dissipated by the conductor per unit length, T is the conductor mechanical tension and K_1 is a factor of proportionality. It has been demonstrated that the values of the exponents α, β and γ may depend upon the method used for the measurements as described by CIGRE SC22-WG11-TF1 (1998).

Conductor self-damping can alternatively be expressed in terms of a free-field loss factor η_c as described by Noiseux (1991) who proposed similarity laws for internal damping of stranded cables in transverse vibrations. Hardy and Leblond (1995) reviewed the pioneering work of Noiseux and proposed extended similarity laws which, in principle, are applicable to all multi-layer aluminium conductors:

$$\eta_c = K_2 \frac{(EI)_0}{m} \frac{y_{\max}^{0.44} f^{2.63}}{\sigma_{al}^{2.76}} \tag{5}$$

where $(EI)_0$ is the conductor bending stiffness, σ_{al} is the nominal static longitudinal stress in the aluminium layers of the conductor and K_2 is a factor of proportionality. As the bending stiffness $(EI)_0$ of most ACSR conductors depends only weakly on steel core size, it is roughly proportional to d_4 and Eq. (5) may be approximated by:

$$\eta_c \cong K_3 \frac{d^4}{m} \frac{y_{\max}^{0.44} f^{2.63}}{\sigma_{al}^{2.76}} \tag{6}$$

where K_3 is another factor of proportionality. On account of the Young's modulus of steel being approximately three times as large as that of aluminium, the nominal static longitudinal stress σ_{al} is defined by Noiseux (1991):

$$\sigma_{al} = \frac{T}{A_{al} + 3A_{st}} \tag{7}$$

where A_{al} is aluminium cross-section and A_{st} is steel cross-section. Noting the approximation:

$$(A_{al} + 3A_{st}) \cong \frac{m}{\rho_{al}} \tag{8}$$

where ρ_{al} is aluminium density, Eq. (7) may be expressed:

$$\sigma_{al} \cong \frac{\rho_{al} H}{m} = \frac{\rho_{al}\, g\, H}{w} \tag{9}$$

where symbol T has been replaced by symbol H, the horizontal tensile load in the conductor, g is the acceleration of gravity and w is the conductor weight per unit length. The ratio H/w in Eq. (9)

is known as the "catenary constant" which is a more practical parameter than σ_{al}. For instance, it is commonly used to determine conductor sag and traveling wave velocity and it has been recently used to define safe design tensions (CIGRE SC22-WG11-TF4 1999) shown in the last column of Table 1. Introduction of Eq. (9) into (6) yields:

$$\eta_c \cong K_4 \frac{d^4}{m} \frac{y_{\max}^{0.44} f^{2.63}}{(H/w)^{2.76}} \tag{10}$$

in which K_4 is still another factor of proportionality.

2.3. Energy balance principle

The EBP identifies an analytical method for assessing the Aeolian vibration level of overhead conductors. The balancing of conductor self-dissipation against wind power input is normally done by means of a computer program in order to predict steady-state vibration amplitudes. The EBP can be simply expressed as follows:

$$\eta_w = \eta_c \tag{11}$$

Introducing Eqs. (1), (2) and (10) into (11) yields :

$$\frac{\rho_a d^2}{2m} fnc_1\left(\frac{y_{\max}}{d}, I\right) = K_4 \frac{d^4}{m} \frac{y_{\max}^{0.44} f^{2.63}}{(H/w)^{2.76}} \tag{12}$$

which may be converted successively to:

$$fnc_1\left(\frac{y_{\max}}{d}, I\right) = 2K_4 \frac{d^{2.44}}{\rho_a} \frac{(y_{\max}/d)^{0.44} f^{2.63}}{(H/w)^{2.76}} \tag{13}$$

and to:

$$\frac{fnc_1\left(\frac{y_{\max}}{d}, I\right)}{(y_{\max}/d)^{0.44}} = \frac{2K_4}{\rho_a} \frac{f^{2.63} d^{2.44}}{(H/w)^{2.76}} \tag{14}$$

The left-hand side of Eq. (14) can be expressed as another function $fnc_2(\ )$:

$$fnc_2\left(\frac{y_{\max}}{d}, I\right) = \frac{2K_4}{\rho_a} \frac{f^{2.63} d^{2.44}}{(H/w)^{2.76}} \tag{15}$$

This simple mathematical transformation is important because $fnc_2(\ )$ depends exclusively on the parameter $\{f^{2.63} d^{2.44}/(H/w)^{2.76}\}$. Hence, for a given wind turbulence intensity, the reduced amplitude $y_{\max}/d$ can be plotted against this parameter, leading to a single, unified response curve applicable to all multi-layer aluminium conductors. However, this parameter is not practical and difficult to handle. Examination of the exponents reveals that they are close to each other and Eq. (15) may be transformed again to yield the following expression:

$$fnc_2\left(\frac{y_{\max}}{d}, I\right) = \frac{2K_4}{\rho_a} \left(\frac{fd}{H/w}\right)^{2.63} \frac{d^{-0.19}}{(H/w)^{0.13}} \tag{16}$$

Now looking at the respective value of the exponents, it is clear that y_{max}/d depends strongly on parameter $fd/(H/w)$ defined here as the reduced frequency (in Hz), which is much easier to handle. Conversely, it depends only weakly on the residual term $\{d^{-0.19}/(H/w)^{0.13}\}$. Hence, reduced parameters y_{max}/d and $fd/(H/w)$, when plotted together at a given wind turbulence intensity I, should lead to a unified vibration curve applicable to all multi-layer aluminium conductors strung at any practical tension.

3. Results

3.1. Theoretical results

In order to validate this unifying process, the calculated response of two different ACSR conductors (Bersfort and Ibis), with characteristics as shown in Table 2, is presented here at 15% wind intensity of turbulence. Using the probabilistic model described by Leblond and Hardy (2000), the maximum antinode amplitude y_{max} is calculated as a function of frequency f as shown in Fig. 2 where six curves of vibration amplitudes are depicted, three for each conductor strung at $H/w =$ 1000, 1500 and 2000 m respectively. For comparison purpose, these results are presented again in Fig. 3 in terms of the two reduced parameters leading to six well-superposed curves which span different ranges of the reduced frequency parameter. It is quite obvious from the graph that the reduced parameters actually unify the calculated results.

3.2. Full-scale test line results

Several undamped single ACSR, AAAC and ACAR conductors strung at different tensions were

Table 2 Conductor characteristics

	Bersfort	Ibis	Carillon	Peace River	Bersimis	ACAR 1300	ACSR (84/19)	AAAC (61/0)
Type	ACSR	ACSR	ACSR	ACSR	ACSR	ACAR	ACSR	AAAC
Stranding	48/7	26/7	42/7	48/7	42/7	18/19	84/19	61/0
Overall diameter (mm)	35.6	19.9	30.5	24.1	35.1	33.3	41.1	40.7
Mass (kg/m)	2.369	0.814	1.648	1.091	2.181	1.816	3.13	2.70
Rated Tensile Strength (kN)	180.1	72.5	118.0	87.5	154.0	145.5	244	245
Outer wire material	Al EC-H19	Al EC-H19	Al EC-H19	Al EC-H19	Al EC-H19	Al EC-H19	Al EC-H19	Al 6201-T81
Outer wire diameter (mm)	4.27	3.14	3.98	2.90	4.57	4.76	3.73	4.52
Reinforcing wire material	Steel	Steel	Steel	Steel	Steel	Al 6201-T81	Steel	–
Reinforcing wire diameter (mm)	3.32	2.44	2.21	2.25	2.54	4.76	2.24	–
Aluminium cross-section (mm^2)	686.5	201.4	521.2	316.1	689.5	658.4	920	980
Total cross-section (mm^2)	747.1	234.2	548.0	344.0	725.0	658.4	995	980

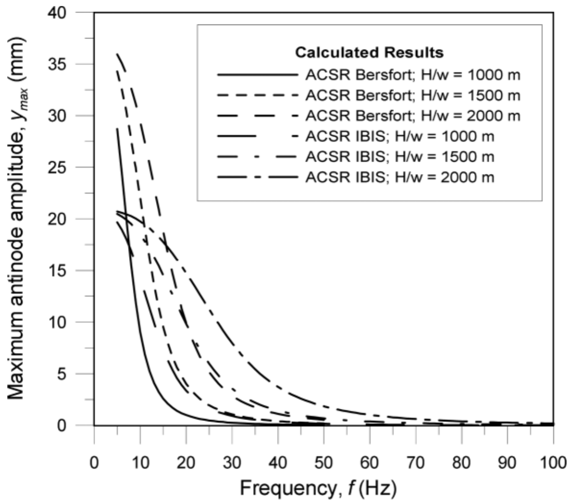

Fig. 2 Calculated results: maximum antinode amplitude as a function of frequency

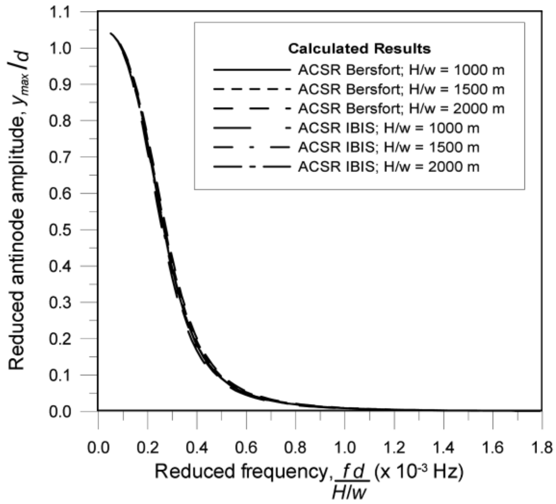

Fig. 3 Calculated results: reduced antinode amplitude as a function of reduced frequency

tested at the former full-scale test line in Magdalen Islands (Quebec, Canada) which was briefly described by Houle, *et al.* (1987). The test line was built on a flat terrain close to the sea which favours low-turbulence wind regimes. The average turbulence level over the site was about 15% which corresponds to terrain #2 in Table 1. The test line consisted of three suspension spans of 274, 366 and 457 m respectively and two anchor spans of 244 m. The test duration was about six to eight weeks to ensure that the conductors had been exposed to a wide variety of winds either from the point of view of velocity or direction.

In order to further validate this unifying approach, the measured response curves drawn from those tests (Hardy, *et al.* 1996) are depicted in Fig. 4 with an average unified response curve derived from Fig. 3. A total of six ACSRs, one ACAR and one AAAC having diameter ranging from 24.1 to 41.1 mm (see Table 2) and tensile loads H/w ranging from 1440 to 2326 m is depicted in Fig. 4. This certainly represents a sound test line data base to validate the unifying approach. On account of the expected scatter in the results from such field tests, the agreement is shown to be good. Such scatter is mainly related to the variability of some parameters over the test period. For instance, the mechanical tension depends on the air temperature which is obviously not constant during the tests, and wind turbulence intensity shows a great deal of dispersion during light to moderate winds associated with Aeolian vibrations (CIGRE SC22-WG11-TF4 1999). However, Fig. 4 shows that the reduced parameters satisfactorily unify test line results thus validating the proposed unifying process.

3.3. Generalized results

From Eq. (16), it can be seen that the reduced antinode amplitude depends essentially on the reduced frequency and wind turbulence intensity. In order to generalize the results to the largest possible extent, only four unified response curves are depicted in Fig. 5, corresponding to the four terrain categories described in Table 1. It may be noted that the scatter of the results depicted in Fig.

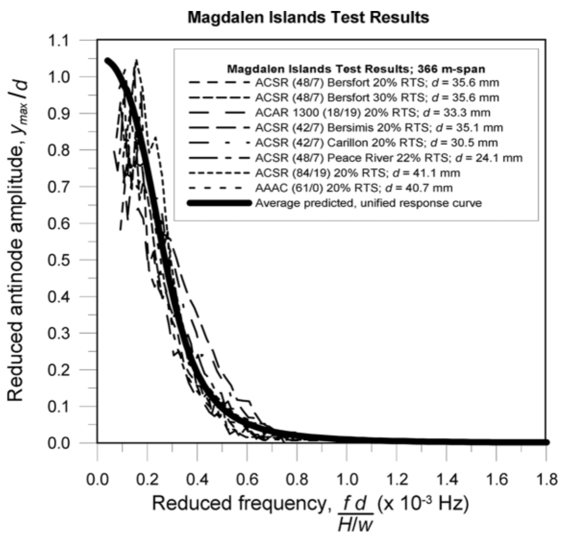

Fig. 4 Magdalen Islands test results: reduced antinode amplitude as a function of reduced frequency

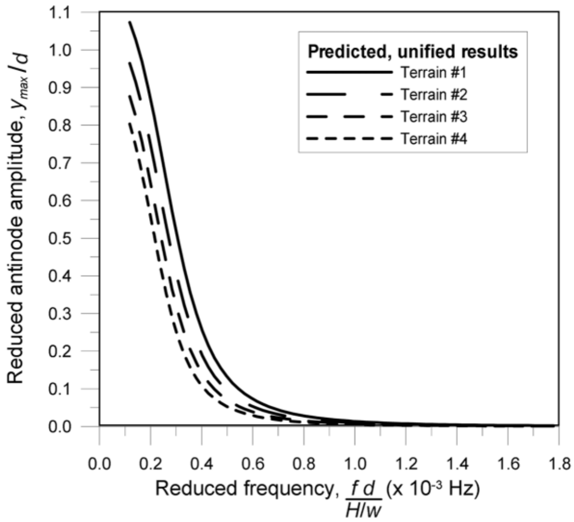

Fig. 5 Predicted, unified results: reduced antinode amplitude as a function of reduced frequency

5 is similar to the one appearing in Fig. 4.

These four unified response curves may be considered as sort of “universal curves” to assess the vibration response of any undamped single conductor of any diameter, strung at any practical tension. The predicted maximum, nominal bending stress at suspension clamp can be calculated by means of the Poffenberger-Swart formulation (EPRI 1979) :

$$\sigma_{a,\,\max} = \pi d_a E_a \sqrt{\frac{m}{EI_{\min}}}\, f\, y_{\max} \tag{17}$$

in which d_a is the outer-layer wire diameter, E_a is Young’s modulus for the outer-layer wire material and $EI_{\min}$ is the minimum flexural rigidity based on the assumption that each individual wire flexes independently of the others. Eq. (17) shows that the maximum bending stress is proportional to the product $f\,y_{\max}$ which can be calculated from the unified response curves as a function of frequency. Assessment of vibration severity may be investigated by comparing the maximum predicted bending stress with the fatigue endurance limit of the conductor at the suspension clamp. According to one popular approach, vibration levels are regarded as completely safe if they do not exceed the so-called conductor endurance limit which stands at 22 MPa for ACSR and ACAR conductors and at 15 MPa for AAAC conductors (EPRI 1979).

4. Discussion

The dimensionless reduced antinode amplitude $y_{\max}/d$ comes out naturally but the reduced frequency parameter $\{f\,d/(H/w)\}$ is new and represents the key parameter for this unifying approach. According to the Strouhal relationship, it is worth noting that $\{f\,d/(H/w)\}$ is proportional to the ratio $\{V/(H/w)\}$ where V is the component of wind speed normal to the conductor, which is obviously independent of conductor characteristics while H/w is a parameter rating the effect of tension on conductor self-damping. Hence, an increase in the conductor tension H/w has the same effect on the reduced antinode amplitude as a proportional decrease in the normal component of wind speed V. This is an important conclusion because the "fluid" parameter V and "structural" parameter H/w are now linked together through the reduced frequency parameter and their respective influence upon the reduced antinode amplitude may be easily assessed.

The quality of the unification is independent of the wind power input expressed in Eq. (16) as a general function $fnc_2(\ )$ but depends solely on the values of the exponents shown in Eq. (15). The closer are these values, the better is the unification. Wind power input affects only the amplitude level of the unified curves, not their unification. The above unifying process may be extended to other self-damping rules as reported by a number of investigators to predict the energy dissipation of conductors of the same family. A comparison of exponents α, β and γ defined in Eq. (4) was presented in an Electra paper (CIGRE SC22-WG11-TF1 1998). It was shown that the most exacting measurement methods lead to empirical rules with $\alpha \cong 2.4 - 2.5$, $\beta \cong 5.5$ and $\gamma \cong 2.7 - 2.8$ which are close to the present values ($\alpha = 2.44$, $\beta = 5.63$ and $\gamma = 2.76$) derived from Eq. (5). Therefore, a good quality of unification may be expected from the use of those self-damping rules as well.

5. Conclusions

A unified way for calculating vortex-induced vibrations (i.e. Aeolian vibrations in transmission line parlance) of undamped single conductors has been presented. By means of a simple mathematical transformation, a reduced antinode amplitude parameter and a reduced frequency parameter were identified to unify the predicted vibration response to the largest possible extent. One advantage of this process is to unify as well the presentation of the results from a full-scale test line, which in turn can be used to validate the results of any computer program.

This unifying process paves the way towards the use of "universal curves" for predicting Aeolian vibration response of undamped single overhead conductors. In this regard, the final results are expressed by means of only four different curves pertaining to four different terrain characteristics. These curves may be used to assess the vibration response of any undamped single, multi-layer aluminium conductor of any diameter, strung at any practical tension.

References

Brika, D. and Laneville, A. (1996), "A laboratory investigation of the aeolian power imparted to a conductor using a flexible circular cylinder", *IEEE Transactions on Power Delivery,* **11**(2), 1145-1152.

CIGRE Study Committee 22 - Working Group 11 - Task Force 1 (1998), "Modelling of aeolian vibration of single conductors : assessment of the technology", *Electra*, (181), 52-69.

CIGRE Study Committee 22 - Working Group 11 - Task Force 4 (1999), "Safe design tension with respect to aeolian vibrations. Part 1 : Single unprotected conductors", *Electra*, (186), 52-67.

CIGRE Study Committee 22 - Working Group on Mechanical Oscillations (1979), "Guide on conductor self-damping measurements," *Electra,* (62), 79-90.

Electric Power Research Institute (1979), *Transmission Line Reference Book - Wind-Induced Conductor Motion*, Palo Alto, Chapter 3.

Hardy, C., Leblond, A., Goudreau, S. and Cloutier, L. (1995), "Review of models on self-damping of stranded cables in transverse vibrations", *Proceedings of the 1st Int'l Symposium on Cable Dynamics*, Liège, 61-68.

Hardy, C., Noiseux, D.U., Leblond, A., Brunelle, J. and Van Dyke, P. (1996), "Modelling of single conductor-damper system response - Volume 1 : Theoretical and validation manual", CEA project 372 T 823.

Houle, S., Hardy, C., Lapointe, A. and St-Louis, M. (1987), "Experimental assessment of spacer-damper performance with regard to control of wind-induced vibrations of high voltage transmission lines", *IEEE/ CSEE Joint Conference on High Voltage Transmission Systems in China*, Beijing, China, October.

IEEE Standard 563 (1978), "IEEE guide on conductor self-damping measurements".

Leblond, A. and Hardy, C. (2000), "Assessment of safe design tension with regard to aeolian vibrations of single overhead conductors", *Proceedings of the ESMO Conference*, Montréal, October, 202-208.

Leblond, A. and Hardy, C. (2003), "A unified way for presenting aeolian vibration response of single undamped overhead conductors", *Proceedings of the Fifth International Symposium on Cable Dynamics*, Santa Margherita Ligure, Italy, September, 263-270.

Noiseux, D.U., Houle, S. and Beauchemin, R. (1988), "Transformation of wind tunnel data on aeolian vibrations for application to random conductor vibrations in a turbulent wind", *IEEE Transactions on Power Delivery*, **3**(1).

Noiseux, D.U. (1991), "Similarity laws of the internal damping of stranded cables in transverse vibrations", *Proceedings of the IEEE PES*, Trans. & Distr. Conf., Dallas, September.

Rawlins, C.B. (1982), "Power imparted by wind to a model of a vibrating conductor", Report no 93-82-1, Electrical Products Div., Alcoa Laboratories, Alcoa Conductor Products, Massena.

Rawlins, C.B. (1998), "Model of power imparted to a vibrating conductor by turbulent wind", Alcoa Conductor products company, Technical Note no 31.

GS